Journal of Food Engineering 303 (2021) 110592

Contents lists available at ScienceDirect

Journal of Food Engineering

journal homepage: http://www.elsevier.com/locate/jfoodeng

Modelling ice growth and inclusion behaviour of sucrose and proteins during progressive freeze concentration

Jan Eise Vuist, Rikke Linssen, Remko M. Boom, Maarten A.I. Schutyser *

Laboratory of Food Process Engineering, Wageningen University and Research, 4 P.O. Box 17, 6700, AA, Wageningen, the Netherlands

ARTICLE INFO

Keywords:
Progressive freeze concentration
Solute inclusion
Sucrose
Whey protein
Dewatering

ABSTRACT

This study focused on modelling ice growth and solute inclusion behaviour during progressive freeze concentration of sucrose, soy protein, and whey protein. Experiments were conducted in a small stirred tank set-up and ice growth was modelled using mass and heat balances. Solute inclusion was estimated using an intrinsic distribution coefficient. For sucrose solutions, the intrinsic distribution coefficient is proposed dependent on the initial and critical concentrations, where the last is related to the fast increase in viscosity and decrease in diffusivity when the solution approaches glass transition. Predictions were found in agreement with experimental data, except when dendritic ice growth was observed. Solutions of whey and soy proteins behaved differently due to their large difference in solubility. These proteins also showed different inclusion behaviour compared to sucrose, due to lower freezing point depression and lower concentrations far away from glass transition.

1. Introduction

Freeze concentration is the process to concentrate aqueous streams by the removal of water as ice crystals after cooling the stream to its freezing point. The main advantage of freeze concentration over concentration by evaporation is that heat sensitive components are not affected at the low temperatures in the process (Berk, 2009; Sánchez et al., 2011; Auleda et al., 2011). There are three different approaches to carry out freeze concentration, i.e. suspension freeze concentration, block freeze concentration and progressive freeze concentration. In suspension freeze concentration the ice crystals are grown in suspension and are removed through a continuous wash filter This process is already available on an industrial scale (Sánchez et al., 2011; Kadi and Janajreh, 2017). In block freeze concentration the solution is completely frozen and then selectivily thawed to remove the concentrate (Moreno et al., 2014; Petzold et al., 2015). In progressive freeze concentration the ice is grown as a layer on a heat exchanger surface. This process is till now mostly investigated at lab scale and some at pilot scale, although some small scale industrial units with a maximum capacity of around 50 l exist and a larger scale unit (100 l) is under development. (Rane and Jabade, 2005; Miyawaki et al., 2005; Meiwa Co. Ltd, 2018). To scale this technology ultimately to an industrially relevant scale and apply it to relevant product streams, more insight is required in the dynamics of the process, which requires both experimental and modelling work.

Progressive freeze concentration involves partial freezing of the fluid on the surface of a heat exchanger (Halde, 1980; Liu et al., 1997). Forced convection reduces concentration polarisation close to the ice surface and thus lowers the amount of solute inclusions into the ice (Vuist et al., 2020). Progressive freeze concentration is operated as a batch process. When the ice layer has a specified maximum thickness and thus the solution has reached the desired concentration, the operation is ended by draining the system. Subsequently the ice is melted to collect the water from the concentrate. If a higher concentration factor is desired, a second progressive freeze concentration step may be applied to the concentrate.

The process of progressive freeze concentration has been studied for various equipment designs. Generally, for minimum solute inclusion in the ice layer, high agitation and low freezing rates are required. Flesland (1995) used an open system with the liquid flowing over a cooling plate and observed that concentration of sucrose solutions could be realised albeit the desired recovery was only achieved at low ice growth rates and by applying a multi-step freeze concentration process (Flesland, 1995; Ratkje and Flesland, 1995). Liu et al. (1997) used a cylinder submerged in a cooled ethanol bath to concentrate glucose solutions. Later, this system was scaled up to a closed tubular device (Miyawaki et al., 2005). In this device, coffee, tomato juice, and sucrose were concentrated, which demonstrated the potential of progressive freeze concentration to relevant streams in food industry. Raventós et al.

* Corresponding author.
E-mail address: maarten.schutyser@wur.nl (M.A.I. Schutyser).

https://doi.org/10.1016/j.jfoodeng.2021.110592
Received 12 November 2020; Received in revised form 26 February 2021; Accepted 15 March 2021
Available online 20 March 2021

(2007) used a setup based on a falling film and Ojeda et al. (2017) used a setup consisting of a stirred tank with cooled walls. They applied freeze concentration to sucrose solutions and concluded that the eutectic point was the limiting factor for freeze concentration. However, sucrose solutions are known for their supersaturation and show no eutectic concentration behaviour (van der Sman, 2016, 2017).

To allow scaling of film freeze concentration towards industrial scale, modelling can be used to design larger-scale freeze concentration processes and to estimate the efficiency and economics at this scale. In several previous studies models were developed for the film freeze concentration process. Ratkje and Flesland (1995) assumed the growth rate of ice to be constant and derived that inclusions may be prevented when the ice growth rate is below a maximum threshold determined by the temperature difference between the ice front and the cooling surface and the diffusion rate of the solute (Scholz, 1993; Scholz et al., 1993; Flesland, 1995; Ratkje and Flesland, 1995). Auleda et al. (2011) proposed a modelling approach for a falling film freeze concentrator based on the work of Chen and Chen (2000), who employed a semi-empirical correlation based on freezing point depression, ice growth rate and the liquid velocity. Miyawaki et al. (1998) proposed an intrinsic distribution coefficient (K_0) to predict solute inclusion during progressive freeze concentration. This intrinsic distribution coefficient is the ratio between the solute concentration in the ice and the solute concentration in the solution at the boundary, when the boundary moves infinitesimally slowly (eq. (1)).

$$K_0 = \frac{C_s}{C_i} \tag{1}$$

The intrinsic distribution coefficient K_0 is in fact an empirical parameter that can be obtained from freeze concentration experiments with a specific solute. Gunathilake et al. (2013) observed that K_0 is concentration dependent. Gu et al. (2006) related the intrinsic distribution coefficient to the osmotic pressure, which in it self is directly related to the water activity of the solution. This worked well for calculating the coefficient for single component system containing salt, however for glucose and dextran mixtures they found that the viscosity had a large influence on the intrinsic distribution coefficient. Chen and Chen (2000) related the distribution coefficient to the freezing point depression via a semi-empirical relationship and found the correlation to fit well for falling film freeze concentration and suspension freeze concentration. They expanded upon this work to determine the maximum allowable freezing rate and to account for different geometries of the cooling systems (Chen et al., 2015).

The aim of this work is to develop a coupled heat and mass transfer model to describe the freeze concentration process including solute inclusion. Specifically, we investigate the relation of the intrinsic distribution coefficient (K_0) to the phase behaviour of the solute and the solvent to predict solute inclusion. We hypothesise that K_0 is related to the ratio of the concentration of the solution and a critical concentration related to the glass transition. We compare freeze concentration experiments and model predictions for protein and sugar solutions. Measurements were done on lab scale in which the ice growth rate and solute inclusion were both analysed.

2. Theory

2.1. Ice growth

The average ice growth rate on the cooling plate follows from the energy balance over the ice boundary (eq. (2)) Rane and Jabade (2005).

$$\frac{dM_{ice}}{dt} = \frac{(q_{ice} - q_{fp})A_{fp}}{\Delta H_{fus}} \tag{2}$$

$$q_{ice} = h(T_l - T_{fp}) \tag{3}$$

$$q_{fp} = h_{ov,i}(T_{fp} - T_{coolant}) \tag{4}$$

We assume that the ice growth is proportional to the excess of heat removed via the ice layer (eq. (4)) minus the heat transported towards the ice boundary from the fluid bulk (eq. (3)). If we assume that the ice is growing uniformly, the ice growth rate can be derived via the ice density (eq. (5)). The heat of fusion, ΔH_{fus}, was assumed to be equal to that of water (333.5 kJ/kg).

$$v_{ice} = \frac{dL_{ice}}{dt} = \frac{q_{ice} - q_{fp}}{\Delta H_{fus}\rho_{ice}} \tag{5}$$

2.2. Solute inclusion

The concentration effect in film freeze concentration is caused by exclusion of the solute from the ice. However the exclusion of the solute is not perfect and this leads to solute inclusion. This can be expressed as an average distribution coefficient, K (eq. (6)). The average distribution coefficient can be measured after a freeze concentration experiment by analysing the composition of the fluid (C_l) and the ice phase (C_s), respectively (Fig. 1). Due to concentration polarisation the average distribution coefficient is not equal to the intrinsic distribution coefficient (eq. (1)) (Burton et al., 1953b).

$$K = \frac{C_s(t)}{C_l} \tag{6}$$

$$K_0 = \frac{C_s}{C_i} \tag{7}$$

The concentration polarisation above the ice surface can be described with a mass balance over the hydrodynamic boundary layer (eq. (8)).

$$-D\frac{dC}{dx} + v_{ice}C = v_{ice}C_s \tag{8}$$

The frame of reference for this mass balance is the ice surface which is defined to be at $x = 0$. Ice growth leads to a flux of water with speed v_{ice} into the ice. C_s is the concentration of solute in the ice, C is the

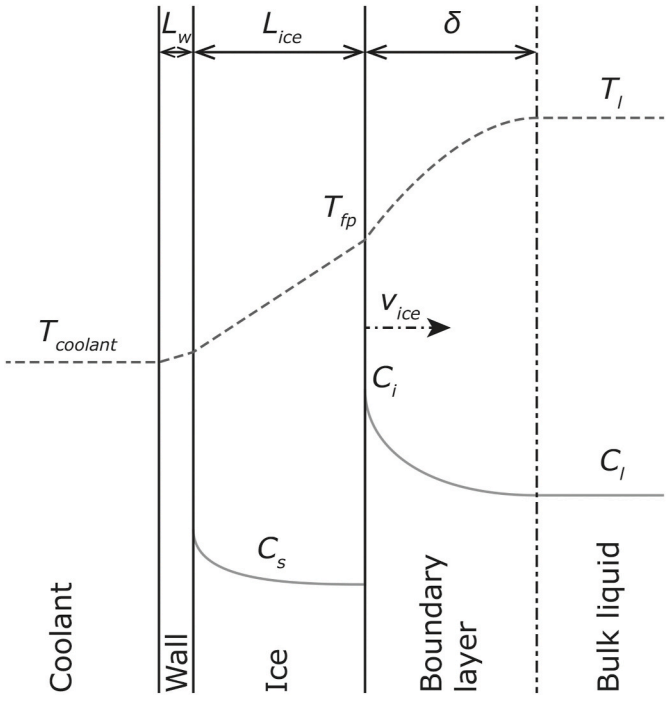

Fig. 1. Schematic drawing of the temperature and concentration profiles near the cold wall. For visualization the system is rotated with 90°.

concentration in the boundary layer, and D is the diffusion coefficient of the solute in the solvent. The boundary conditions for this equation are $C = C_i$ at $x = 0$ (the concentration in the liquid phase) and $C = C_l$ at $x = -\delta$ where δ is the boundary layer thickness. When these boundary conditions are used eq. (8) can be integrated to obtain eq. (9).

$$\frac{C_i - C_s}{C_l - C_s} = \exp\left(\frac{v_{ice}\delta}{D}\right) \tag{9}$$

When combining eq. (9) with the definition for the intrinsic distribution coefficient and replacing D/δ by the mass transfer coefficient k, a practical expression is obtained for the concentration of the solute at the ice boundary (eq. (10)).

$$C_s = \frac{\exp\left(\frac{v_{ice}}{k}\right) C_l}{\exp\left(\frac{v_{ice}}{k}\right) + \frac{1}{K_0} - 1} \tag{10}$$

2.3. Intrinsic distribution coefficient

The intrinsic distribution coefficient, K_0, is proposed by Burton et al. (1953b) as the ratio of the concentration of solute in the ice, C_s and that in the liquid at the interface, C_i. This ratio converges to a constant value when the temperature of the ice approaches the freezing temperature (Burton et al., 1953a, b). Gunathilake et al. (2013) showed that for sucrose systems the intrinsic distribution coefficient depends on the solution concentration (C_l). Gu et al. (2006) observed this dependence also for different salts and glucose and related the intrinsic distribution coefficient to the osmotic pressure, although they could not explain the behaviour of glucose at 20%.

$$K_0 = \frac{C_l}{C_{critical}} \tag{11}$$

$$C_{critical} = f\left(T_m, T'_g\right) \tag{12}$$

As small carbohydrates like sucrose tend to be supersaturated at low temperatures, rather than allow crystallization of the carbohydrate, we cannot use a eutectic point, which normally should lead to the maximum degree of freeze concentration. We therefore propose that the value of K_0 (eq. (11)) is, for small carbohydrates, dependent on the ratio between the solute concentration in the liquid and the concentration determined by a margin above where the apparent glass temperature (T'_g) meet the solidus line (T_m), this is deemed the critical concentration (eq. (12)) (van der Sman and Mauer, 2019; Roos and Karel, 1991a, b). For sucrose this value was determined to be 0.62 kg/kg.

The ultimate end point for freeze concentration would be the point where the freezing line would cross the line of the glass temperature Fig. 2. At this point a maximally freeze concentrated system would be obtained (Roos and Karel, 1991a, b). In the glassy state a domain of pure ice and small glassy domains of the maximally freeze concentrated sugar solution would co-exist. Since the diffusion coefficient at the glass temperature is effectively zero, this would imply that the ice would have the exact same composition as the solution, as the solutes cannot diffuse away from the freezing frontier anymore. However, before reaching the glass transition temperature, we have to consider the rapidly increasing viscosity when approaching this solidification point (Williams et al., 1955). This increase in viscosity for sucrose solutions becomes relevant when the solution is super-saturated, especially when working at low temperatures during freeze concentration (Kauzmann, 1948). It leads to significant reduction of the mass transfer rate in the boundary layer and as a result the solute concentration gradient in the boundary layer will increase. Due to the higher concentrations, the inclusion rate increases and a less effective separation is achieved. In this case the intrinsic partition coefficient (eq. (11)) can be considered to give an indication of the remaining capacity for a carbohydrate system to be concentrated.

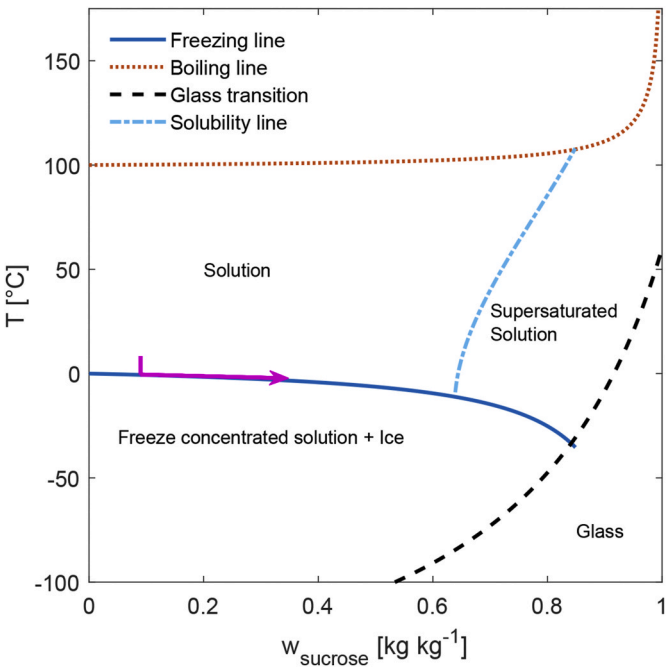

Fig. 2. State diagram of sucrose after Roos (2010); van der Sman (2017). The purple arrow indicates the trajectory of the solution during progressive freeze concentration. (For interpretation of the references to colour in this figure legend, the reader is referred to the Web version of this article.)

3. Material and methods

3.1. Description of the progressive freeze concentrator

A schematic drawing of the lab scale film freeze concentrator, used in this paper, is shown in Fig. 3. A similar set-up has been used in previous work (Vuist et al., 2020), compared to this system the volume has been reduced by reducing the height of the cylinder to 90 mm. The system consists of a vessel that contains the solution that needs to be concentrated, separated with a metal plate from a chamber that contains circulating fluid, temperature-controlled by an external cryostat. The experiments are started by first freezing a droplet (0.1 ml) of distilled water to prevent supercooling of the liquid and to avoid spontaneous bulk crystallization of a supercooled liquid. As soon as the droplet is frozen, the precooled liquid feed is added through a funnel. After the vessel has been filled completely, stirring is started. After the experiment the concentrated liquid is drained from the tank and the ice layer is wiped dry with a paper tissue. Subsequently the ice layer is melted. Samples were taken from the liquid at $t = 0$ and at t = end, plus a sample was taken from the molten ice. The samples were stored frozen until analysis. For the concentration experiments four different cooling programmes were used: two constant temperature programmes at 5 °C or 10 °C below the freezing point of the solution for 1 h, only applied to the soy protein concentrate, and two decreasing temperature programmes starting 2.5 °C below the freezing point and then decreasing by 0.1 °C/min or 0.5 °C/min for 1 h applied to all solutions. The freezing points of the solutions have been calculated using the Clausius-Clapeyron equation (eq. (13)).

$$\ln(1 - x_s) = \frac{\Delta H_{fus}}{\mathrm{R}}\left(\frac{1}{T_{fp,0}} - \frac{1}{T_{fp}}\right) \tag{13}$$

3.2. Materials

Solutions of sucrose, soy protein concentrate (SPC) and whey protein isolate (WPI) solutions were used as feed solutions. Sucrose was

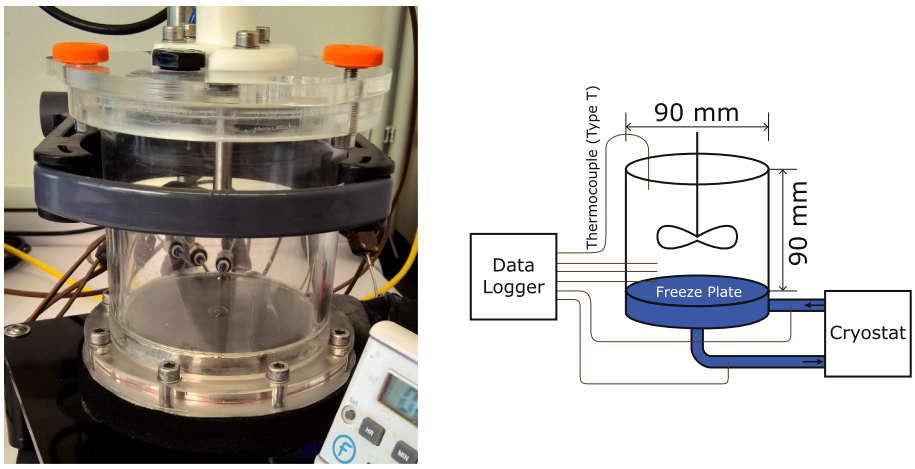

Fig. 3. Picture (left) and schematic representation (right) of the small-scale setup.

obtained from Sigma-Aldrich (USA, BioXtra, purity >99.5%), SPC was obtained from Vitablend (The Netherlands, Unico HS IP, minimum 70% protein), and WPI was obtained from Davisco (Switzerland, BiPro®, purity >97.0%). Sodium phosphate dibasic and sodium phosphate monobasic were obtained from Sigma-Aldrich (USA, at least analytical grade). All solutions were prepared with ultrapure water from a Milli-Q system (Millipore Corporation, United States).

3.3. Methods

3.3.1. Solution preparation

Sucrose and WPI solutions were prepared by dissolving sucrose and WPI in ultrapure water. The solutions were stirred at room temperature until everything was dissolved. The SPC solution was prepared by dissolving the SPC overnight at 4 °C while stirring was applied. The next day the solution was centrifuged for 30 min at 16,000 xG and 4 °C to remove any residual insoluble particles. The supernatant was then collected to be used as the solution in concentration experiments. The solutions were stored at 0 °C in an ice bath until usage the next day.

3.3.2. Ice growth measurement

The ice growth during the freeze concentration of the proteins was monitored by time-lapse pictures taken during the experiment. These pictures were analysed using image analysis software (ImageJ, USA) to determine the ice growth rate (Fig. 4). The width of the front bolt (8.38 mm) in the picture is used as a reference for sizing. With this reference, the ratio of pixels per mm was calculated and thus the ice thickness could be quantified.

3.3.3. Sucrose content

The sucrose content of the sucrose solution was determined using a refractometer (Anton Paar, Abbemat 500, Germany).

3.3.4. Protein content analysis

For both the SPC and WPI samples the dry weight was determined. For this, the samples were placed in pre-weighed cups and dried overnight at 105 °C. The SPC samples were further analysed using the Dumas method. Approximately 10 mg of dry sample was weighed in an aluminium cup and then closed. The nitrogen content was measured (ThermoFisher, FlashEA 1112 series N Analyser, USA) and multiplied with a conversion factor 6.25 to convert the nitrogen content to protein mass. The WPI samples were analysed using HPSEC (Thermo Ultimate 3000 HPLC, ThermoFisher Scientific, USA) on two columns in series (TSKGel G3000SWXL and G2000SWXL, both 5 μm 300 × 7.8 mm) at 30 °C, using UV–Vis detection at 214 nm. The sample size was 10 μl. The feed samples were diluted 10 times with water, the ice fraction samples were used undiluted. The eluent was 30% Acetonitrile in Milli-Q water with 0.1% Trifluoracetic acid. The flow rate of the eluent was 1.5 ml per minute.

3.3.5. Equation solving

The differential equations were solved using a variable order Runge-Kutta method (ode45, Mathworks MATLAB R2019b, USA) (Dormand and Prince, 1980; Shampine and Reichelt, 1997).

3.3.6. Determination of intrinsic partition coefficient

To determine the intrinsic partition coefficient K_0, we express the partition coefficient as function of the intrinsic partition coefficient, the ice growth rate and mass transfer coefficient by rearranging eq. (10) and using the definition of K (eq. (6)) to obtain eq. (18). This equation can again be rewritten into eq. (19) giving a linear relation between $\ln(1/K-1)$ and v_{ice}/k (Pradistsuwana et al., 2003). The mass transfer coefficient, k was determined from the Sherwood relation for stirred tanks (eq. (14) to (17)).

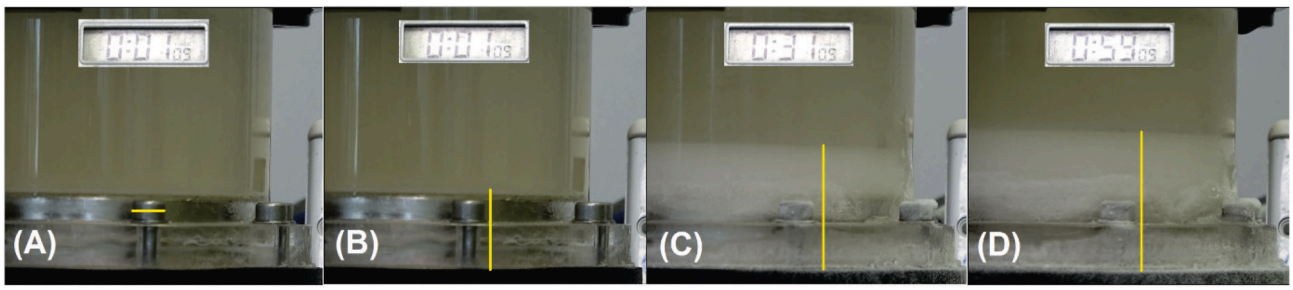

Fig. 4. Method to measure ice growth; (A) width of the bolt, (B) thickness after 1 min, (C) thickness after 31 min, (D) thickness after 59 min.

$$N_{Sh} = \frac{k}{D/L} \tag{14}$$

$$N_{Sh} = 0.36 N_{Re}^{\frac{2}{3}} N_{Sc}^{\frac{1}{3}} \tag{15}$$

$$N_{Re} = \frac{\rho N d^2}{\mu} \tag{16}$$

$$N_{Sc} = \frac{\mu}{D\rho} \tag{17}$$

$$K = \frac{K_0}{K_0 + (1 - K_0)\exp\left(-\frac{v_{ice}}{k}\right)} \tag{18}$$

$$\ln\left(\frac{1}{K} - 1\right) = \ln\left(\frac{1}{K_0} - 1\right) - \frac{v_{ice}}{k} \tag{19}$$

By fitting this linear equation to experimental data obtained at different ice growth rates and/or stirrer rates we can obtain the intrinsic partition coefficient by extrapolating $v_{ice}/k \rightarrow 0$ (Fig. 5).

4. Results and discussion

4.1. Modelling ice growth rate as function of time

We first measured ice thicknesses as a function of time for different conditions and compared those to the predictions by the energy balance (eq. (5)) (Fig. 6). Fig. 6A shows the ice thickness increase for a 4% (w/w) soy protein concentrate solution with a constant plate temperature of −10 °C and a stirring rate of 300 rpm. There is a slight overestimation of the ice growth in the initial phase, but at larger times the agreement is quite good. This slight overestimation of the initial ice growth may be explained by our use of a fixed density in the model, which is critical for calculating the ice thickness (eq. (5)). In the initial phase the growth rate is very high, leading to more inclusions leading to a significantly larger ice volume compared to the ice volume in the model. Fig. 6B shows the ice growth for the same solution stirred at 700 rpm. At this high stirring rate the ice growth is consistently overestimated for the entire process.

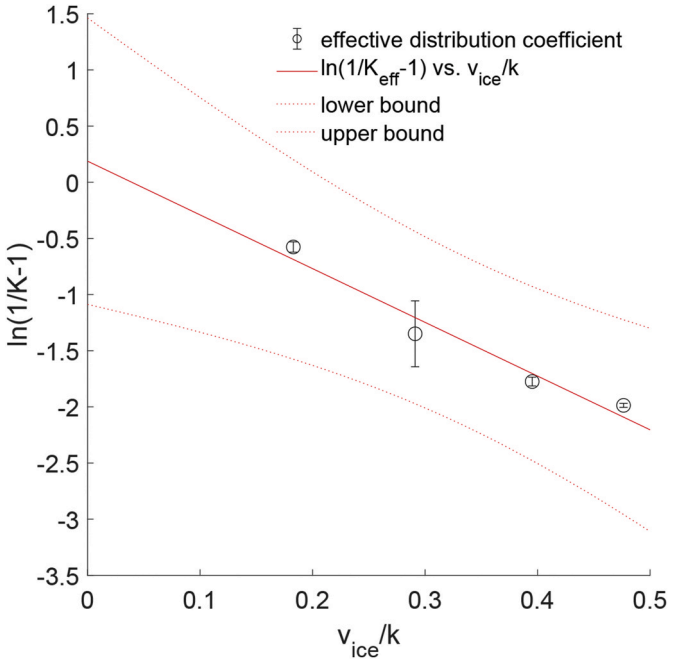

Fig. 5. Result of linear regression on inclusion data obtained for Soy Protein Concentrate.

We expect this is due to the increased heat loss via the side walls of the tank leading to a slowdown of the ice growth in practice. This effect is more pronounced for the −5 °C cooling temperature, because at this temperature relatively more cooling capacity is used for compensating the heat influx from the environment than for ice growth.

In Fig. 6C the ice growth ice is shown using a linear decreasing temperature of the freezing plate with a 4% (w/w) SPC solution. The ice thickness increases approximately in linearly, except for an initial lag, which can be observed for the −0.1 °C/min cooling profile. This lag may be caused by two effects that are not taken into account into the model. First, the gradual cooling of the walls of the cylinder and the heat influx from the environment have not been taken into account, and these effect are relatively large for a small temperature difference between the liquid and the coolant, relative to the heat removed for ice growth. A second aspect is the crystallization kinetics (Myerson et al., 2019). At −0.5 °C/min the lag is not noticeable, as the faster decrease in temperature dominates.

In Fig. 6D, freeze concentration with the same temperature ramps is shown for a 4% (w/w) WPI solution. One may compare with Fig. 6C for a 4% SPC solution. The calculated values for ice height are almost similar. This is expected as both solutions have similar density, viscosity and heat conductivity. However a systematic overestimation is observed for the Whey Protein Isolate solution. This overestimation is probably caused by the ice being purer, as we will show below, and thus the ice has a lower volume than the ice during freeze concentration with SPC since there are less inclusions. For all solutions concentrated the ice growth rate was around 1 μm/s for 0.1 °C/min cooling and 5 μm/s for 0.5 °C/min. These values are inline with the values reported in literature (Miyawaki et al., 2005; Gunathilake et al., 2013; Moreno et al., 2014).

The calculated and measured ice masses after 1 h of freeze concentration are compared in Fig. 7. For the constant cold wall temperature conditions the calculated values are relatively close to the parity line. The calculated values for the 0.1 °C/min decreasing ramp show a similar trend for both SPC and WPI, slightly overestimating the ice mass formed. The calculated values for 0.5 °C/min WPI show a slightly larger overestimation than for the 0.1 °C/min decrease and SPC shows an even larger overestimation. This is probably caused by more solute inclusions. The inclusions of pockets of highly concentrated solution reduce the conductivity (Kestin et al., 1984; Bonales et al., 2017). while the larger volume and thus thickness of the ice layer also reduces the conductance. Both effects slow the ice growth more than predicted by our model that does not include these effects.

4.2. Solute inclusion

Solute inclusion has been modelled according to eq. (10) and is presented in Fig. 8 as the average solute distribution, together with the measured solute inclusion. The solute inclusion with a cooling ramp of 0.5 °C per minute is underestimated for all the solutes. The increased concentration polarisation at a higher ice growth rate causes more inclusion than would be expected from the concentration in the bulk. This increased concentration polarisation may again lead to a more supercooling and thus formation of dendritic ice crystals, which leads to increased solute inclusion (Myerson et al., 2019). The formation of dendritic ice crystals is obviously not taken into account in the current model. The obtained measured inclusions for sucrose are found similar to those reported by Miyawaki et al. (2005). Since the whey protein used in our experiments contains almost no lactose and salts we have found hardly any inclusion of protein in our experiments at low ice growth rates. Sánchez et al. (2011) reported distribution coefficients range from 0.25 to 0.45 depending on the solids concentration.

For the sucrose solutions concentrated with a cooling ramp of 0.1 °C per minute, the solute inclusion for the 6% (w/w) sucrose solution is overestimated while for the other solutions the solute inclusion is underestimated (Fig. 8). This is caused by a larger supercooling at these concentrations. Even though the cooling profile was adjusted for each

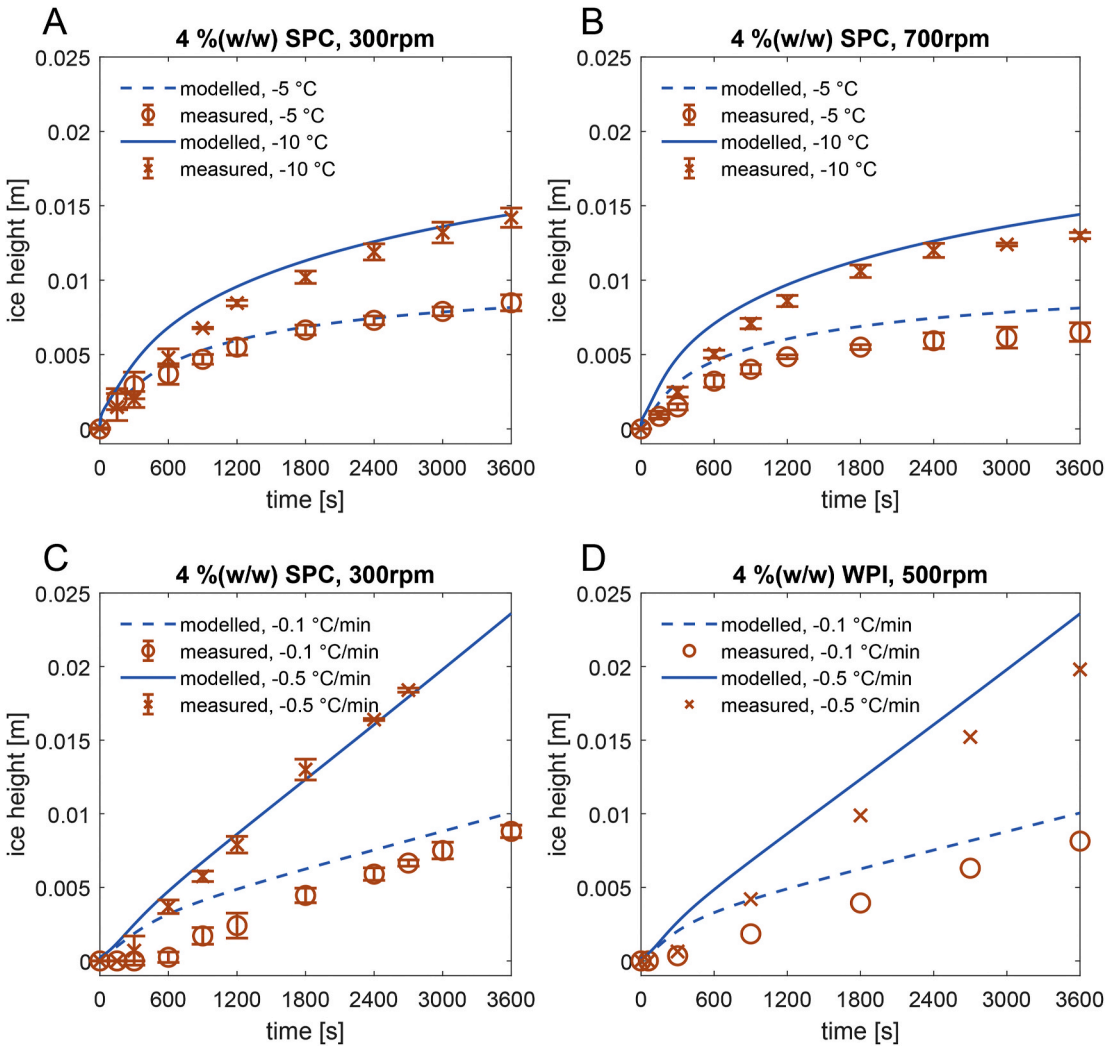

Fig. 6. Modelled and measured ice growth for SPC and WPI at different cooling profiles and different stirring rates for 1 h.

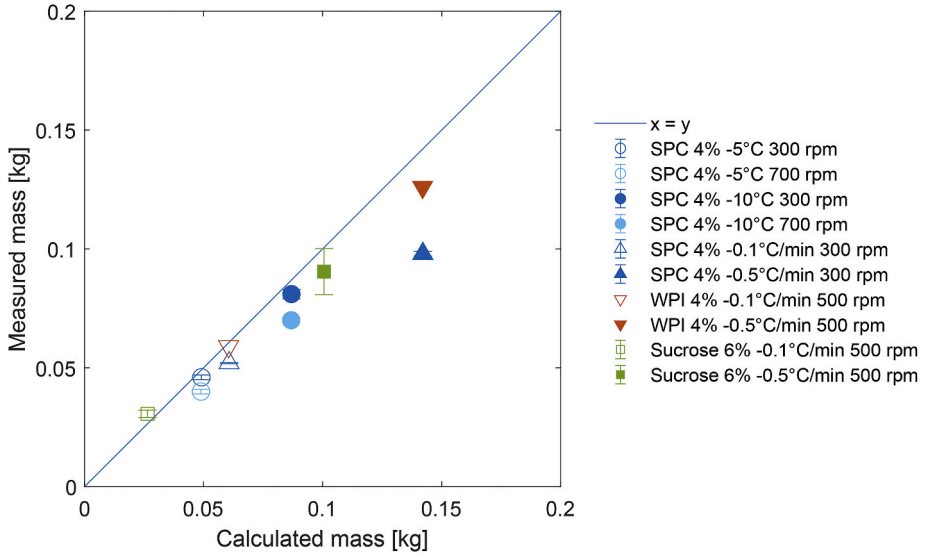

Fig. 7. Parity plot between the calculated ice mass and measured ice mass after 1 h of freeze concentration.

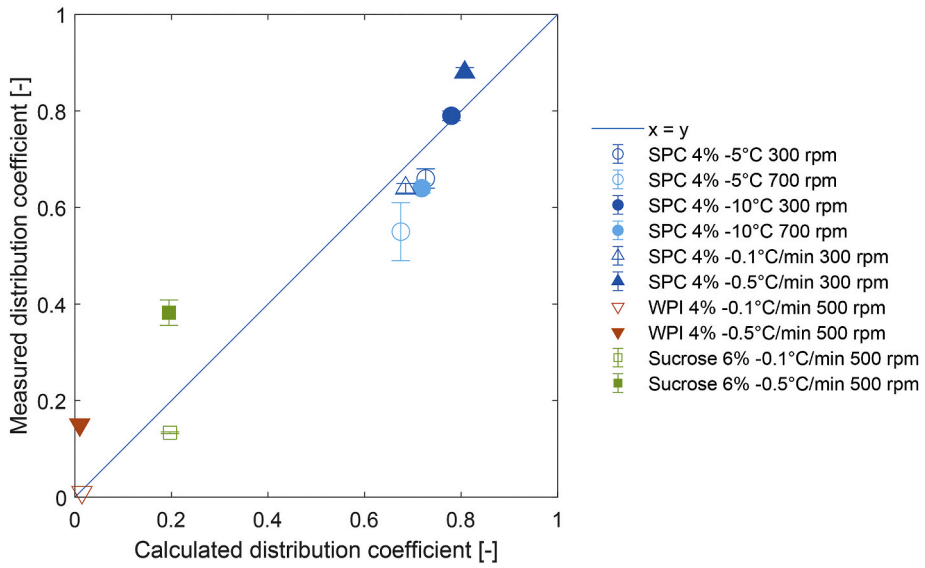

Fig. 8. Parity plot between calculated distribution coefficients and measured distribution coefficients after 1 h of freeze concentration.

solution to yield the same ΔT considering the freezing point depression, the initial temperature could not be adjusted. This causes an initial delay in ice growth and therefore the cooling profile already had progressed to a lower temperature (Fig. 6). This leads to more supercooling near the cold wall resulting in the formation of ice dendrites.

A large difference in inclusion can be noticed between soy protein and whey protein solutions (Fig. 8). Soy protein leads to much inclusion while whey protein gives very low to almost no inclusion. The main difference between the two solutions is the solubility of the proteins (Shen, 1976; Elgedaily et al., 1982). Whey protein isolate contains highly soluble globular proteins (Sánchez et al., 2011). In contrast, SPC consists for a large part of insoluble particles. Compared to soluble proteins, the diffusion rate of particles is negligible, and therefore these particles will be included in the ice. For SPC, this is almost 80% of all proteins. WPI is so well soluble, and can diffuse from the ice freezing front into the bulk solution.

4.3. Outlook to future application of the model and optimization of the process

Even though there are some deviations from the experiments, the model is sufficiently accurate for exploring untested conditions and for optimizing the process. One case of interest would be to optimise the process to reach a certain ice layer thickness, instead of comparing cooling strategies with a fixed end time. This would involve the comparison of the inclusion behaviour between the different cooling rates, towards the same amount of ice generated. Fig. 9 shows the results for a WPI solution at an initial solid content of 4% (w/w) and for sucrose solutions at 6, 18, and 36% (w/w) solid content. Most remarkable is that the level of inclusions is almost constant between the lowest cooling rate (−0.1 °C per minute) and the highest cooling rate (−0.5 °C per minute). This indicates that while there is a higher inclusion rate at higher cooling rates, the averaged level of inclusions per kg of formed ice is nearly constant, While the ice growth rates are ≈ 1 μm/s and 5 μm/s respectively. This means that only the mass transfer near the ice boundary is of influence on the efficiency of progressive freeze concentration (Liu et al., 1997; Vuist et al., 2020). Within the range of the ice growth rate, the distribution coefficient is only weekly dependent on the ice growth rate. The value of K varies from 0.2903 to 0.2935 for a range of ice growth rates between 0 and 10 μm/s.

The model can be used to evaluate the evolution of ice yield and solute inclusion in time for different process conditions. In Fig. 10 the simulation results for 18% (w/w) sucrose are presented. As expected

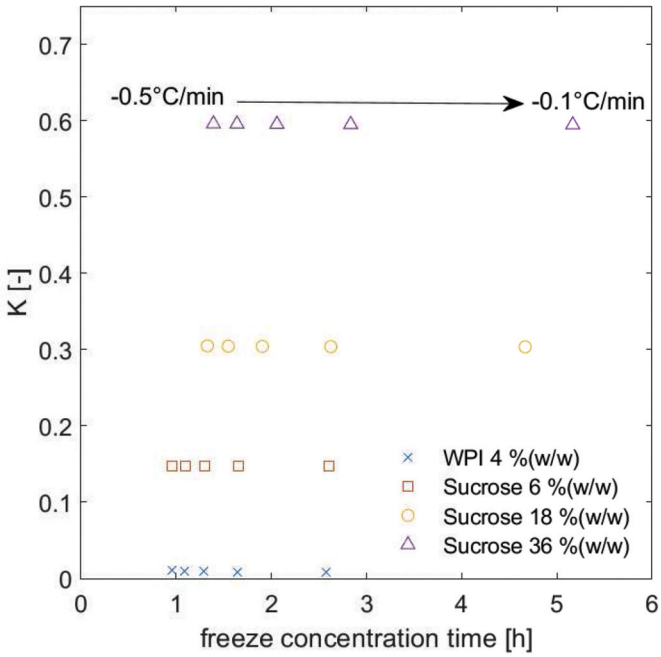

Fig. 9. Simulation results of freeze concentration for varying cooling rates ending at a fixed ice layer thickness (2.25 cm). The effective distribution coefficient as function of time to freeze concentrate till the set ice thickness.

there is a steep initial ice growth followed by a constant freezing rate Fig. 10a. This initial growth is reflected in the effective partition coefficient (Fig. 10b), which starts at a high value; then levels off and then continues to decrease slowly due to the increasing concentration in the bulk fluid (Fig. 10c), which increases faster than the increase in concentration in the ice (Fig. 10d).

An optimum in solute inclusion is shown in Fig. 10d after around 10% of the end time. This could be chosen as an end point for the process when optimizing for the lowest possible level of solute inclusion. The minimum effective distribution coefficient is lower at lower ice growth rates and could be lowered even further, for example by improving the mass transfer rate. However, in practice, the end point can be chosen to be later to allow for a thicker ice layer since the increase of concentration in the ice, and therefore the solute loss, is not steep after this point.

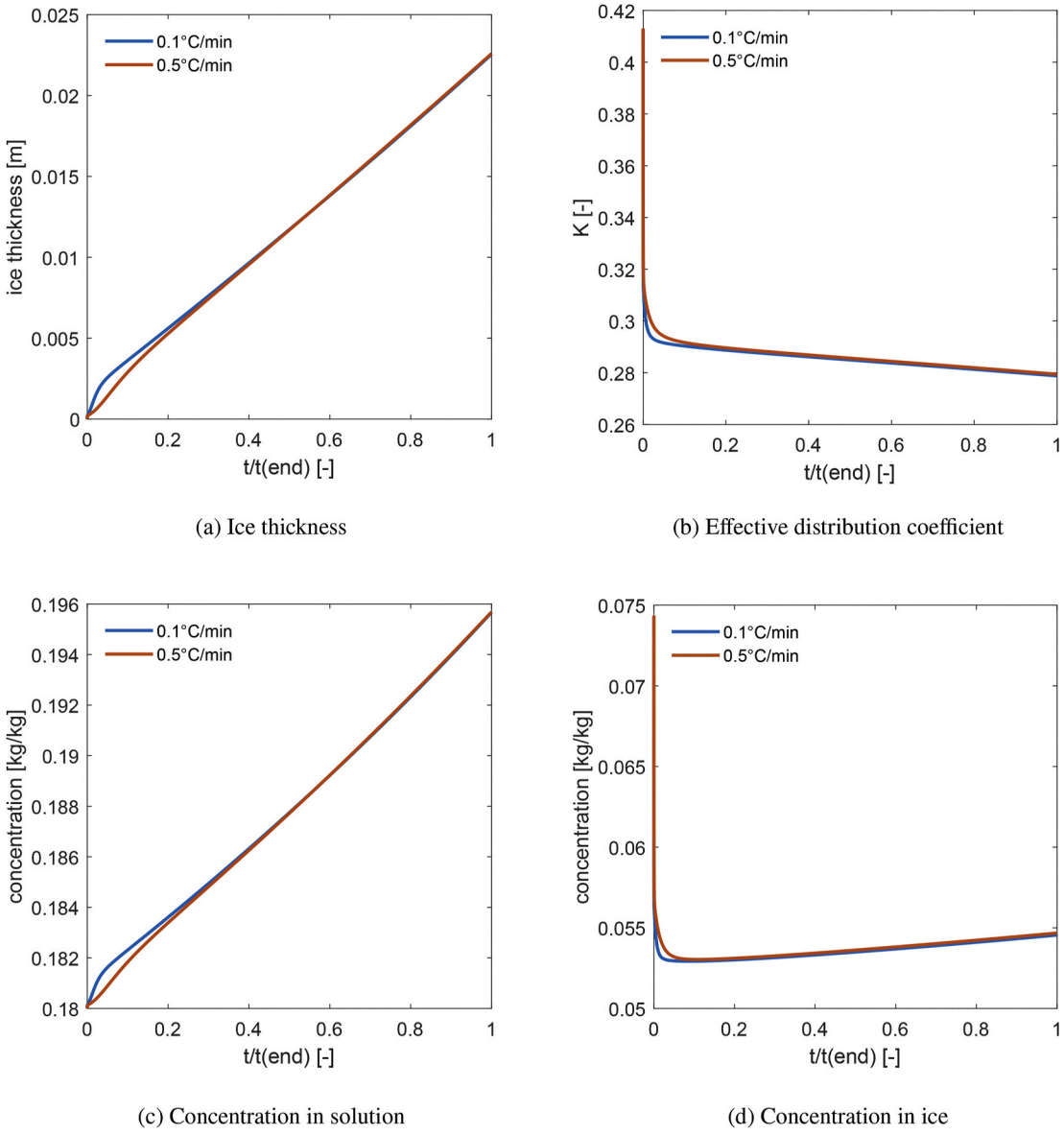

(a) Ice thickness

(b) Effective distribution coefficient

(c) Concentration in solution

(d) Concentration in ice

Fig. 10. Concentration of 18% (w/w) sucrose at two cooling rates, calculated.

This thicker ice layer would allow for a more productive unit. These results also show that the cooling surface to volume ratio should be as high as possible to achieve a high concentration factor in a single step.

5. Conclusion

Progressive freeze concentration was studied using a lab-scale progressive freeze concentrator. A model based on an energy and mass balance was created, using an effective distribution coefficient for solute inclusion. The intrinsic distribution coefficient for sucrose solutions depends on the initial sucrose concentration and on the critical (saturation) concentration, which is probably related to the fast increase in viscosity and reduction in diffusivity when a sucrose solution gets closer to the glass transition. Solutions of proteins behave differently, since their freezing line is flatter, and their solutions in the concentration polarisation layer do not come near their glass transition line. Whey protein isolate, which is well soluble, gives very low inclusions; but soy protein isolate, which mostly consists of small insoluble protein particles gives very large levels of inclusions, up to 80%. The freezing rate has little influence on the achieved effective distribution coefficient, when evaluated at similar amounts of ice produced. The model did indicate a minimum in the level of inclusions, which may be used in the design of the process towards optimal concentration.

Credit author contribution statement

Jan Eise Vuist: Conceptualization of this study, Methodology, Formal analysis, Writing - Original draft preparation. Rikke Linssen: Methodology, Investigation. Remko M. Boom: Writing - Original draft preparation, Supervision. Maarten A.I. Schutyser: Conceptualization, Writing - Original draft preparation, Funding acquisition.

Acknowledgements

This work is an Institute for Sustainable Process Technology (ISPT) project. Partners in this project are TNO, Royal Cosun, Nouryon, Wageningen University and ISPT. This project is co-funded with subsidy from the Topsector Energy by the Ministry of Economic Affairs and Climate Policy.

Nomenclature

ΔH_{fus}	Heat of fusion [kJ kg^{-1}]
δ	Thickness of the boundary layer [m]
μ	Dynamic viscosity [Pa s]
ρ_{ice}	Density of ice [kg m^{-3}]
R	Universal gas constant [J K^{-1} mol^{-1}]
A_{fp}	Area cooling plate [m^2]
C_l	Concentration of solute in solution [kg kg^{-1}]
C_s	Concentration of solute in ice [kg kg^{-1}]
$C_{critical}$	Critical concentration for freeze concentration [kg kg^{-1}]
C_i	Concentration of solute at the ice boundary [kg kg^{-1}]
D	Diffusion coefficient [m^2 s^{-1}]
d	Diameter freeze cell [m]
h	Heat transfer coefficient (liquid boundary layer) [W m^{-1} K^{-1}]
$h_{ov,i}$	Heat transfer coefficient (overall, ice + heat exchanger) [W m^{-1} K^{-1}]
K	Average distribution coefficient [−]
k	Mass transfer coefficient [m s^{-1}]
K_0	Intrinsic distribution coefficient [−]
L	Specific length [m]
L_{ice}	Thickness of ice [m]
L_w	Thickness of the wall [m]
M_{ice}	Mass of ice [kg]
N	Stirring rate [s^{-1}]
N_{Re}	Reynold's number [−]
N_{Sc}	Schmidt's number [−]
N_{Sh}	Sherwood's number [−]
q	Specific heat flow [W m^{-2}]
q_{fp}	Heat transfer from the bulk fluid [W m^{-2}]
q_{ice}	Heat transfer through ice layer [W m^{-2}]
t	Time [s]
T_g	Glass transition temperature [°C]
T_l	Temperature of the liquid [°C]
T_m	Melting temperature [°C]
$T_{coolant}$	Temperature of the coolant [°C]
$T_{fp,0}$	Temperature of the freezing point of pure water [°C]
T_{fp}	Temperature of the freezing point [°C]
v_{ice}	Velocity of the boundary [m s^{-1}]
x	Distance from boundary layer [m]
x_s	Mole fraction of solute [−]

References

Auleda, J., Raventós, M., Hernández, E., 2011. Calculation method for designing a multi-plate freeze-concentrator for concentration of fruit juices. J. Food Eng. 107, 27–35 doi:10.1016/J.JFOODENG.2011.06.006. https://www.sciencedirect.com/science/article/pii/S0260877411003074.

Berk, Z., 2009. Freeze drying (lyophilization) and freeze concentration. Food Process Engineering and Technology. Elsevier, pp. 929–945. https://doi.org/10.1016/B978-0-12-415923-5.00023-X. http://linkinghub.elsevier.com/retrieve/pii/B9780081005224000237.

Bonales, L.J., Rodriguez, A.C., Sanz, P.D., 2017. Thermal conductivity of ice prepared under different conditions. Int. J. Food Prop. 20, 610–619. https://doi.org/10.1080/10942912.2017.1306551 doi:10.1080/10942912.2017.1306551.

Burton, J.A., Kolb, E.D., Slichter, W.P., Struthers, J.D., 1953a. Distribution of solute in crystals grown from the melt. Part II. Experimental. J. Chem. Phys. 21, 1991–1996. http://aip.scitation.org/doi/10.1063/1.1698729. doi:10.1063/1.1698729.

Burton, J.A., Prim, R.C., Slichter, W.P., 1953b. The distribution of solute in crystals grown from the melt. Part I. Theoretical. J. Chem. Phys. 21, 1987–1991. http://aip.scitation.org/doi/10.1063/1.1698728. doi:10.1063/1.1698728.

Chen, P., Chen, X.D., 2000. A generalized correlation of solute inclusion in ice formed from aqueous solutions and food liquids on sub-cooled surface. Can. J. Chem. Eng. 78, 312–319. https://doi.org/10.1002/cjce.5450780205 http://doi.wiley.com/10.1002/cjce.5450780205.

Chen, X.D., Wu, W.D., Chen, P., 2015. An analytical relationship of concentration-dependent interfacial solute distribution coefficient for aqueous layer freeze concentration. AIChE J. 61, 1334–1344. https://doi.org/10.1002/aic.14722 http://doi.wiley.com/10.1002/aic.14722, doi:10.1002/aic.14722.

Dormand, J., Prince, P., 1980. A family of embedded Runge-Kutta formulae. J. Comput. Appl. Math. 6, 19–26. https://www.sciencedirect.com/science/article/pii/0771050X80900133. doi:10.1016/0771-050X(80)90013-3.

Elgedaily, A., Campbell, A.M., Penfield, M.P., 1982. Solubility and water absorption of systems containing soy protein isolates, salt and sugar. J. Food Sci. 47, 806–809. https://doi.org/10.1111/j.1365-2621.1982.tb12719.x doi:10.1111/j.1365-2621.1982.tb12719.x.

Flesland, O., 1995. Freeze concentration by layer crystallization. Dry. Technol. 13, 1713–1739. http://www.scopus.com/inward/record.url?eid=2-s2.0-0001420333&partnerID=tZOtx3y1. doi:10.1080/07373939508917048.

Gu, X., Suzuki, T., Miyawaki, O., 2006. Limiting partition coefficient in progressive freeze-concentration. J. Food Sci. 70, E546–E551. https://doi.org/10.1111/j.1365-2621.2005.tb08317.x doi:10.1111/j.1365-2621.2005.tb08317.x.

Gunathilake, M., Shimmura, K., Miyawaki, O., 2013. Analysis of solute distribution in ice formed in progressive freeze-concentration. Food Sci. Technol. Res. 19, 369–374. https://doi.org/10.3136/fstr.19.369 doi:10.3136/fstr.19.369.

Halde, R., 1980. Concentration of impurities by progressive freezing. Water Res. 14, 575–580. https://www.sciencedirect.com/science/article/pii/0043135480901153 https://linkinghub.elsevier.com/retrieve/pii/0043135480901153. doi:10.1016/0043-1354(80)90115-3.

Kadi, K.E., Janajreh, I., 2017. Desalination by freeze crystallization: an overview. Int. J. of Thermal & Environmental Engineering 15, 103–110. http://iasks.org/wp-content/uploads/pdf/IJTEE-1502004.pdf. doi:10.5383/ijtee.15.02.004.

Kauzmann, W., 1948. The nature of the glassy state and the behavior of liquids at low temperatures. Chem. Rev. 43, 219–256. https://pubs.acs.org/doi/abs/10.1021/cr60135a002. doi:10.1021/cr60135a002.

Kestin, J., Sengers, J.V., Kamgar-Parsi, B., Sengers, J.M.H.L., 1984. Thermophysical properties of fluid H2O. J. Phys. Chem. Ref. Data 13, 175–183. https://doi.org/10.1063/1.555707 doi:10.1063/1.555707.

Liu, L., Miyawaki, O., Nakamura, K., 1997. Progressive freeze-concentration of model liquid food. Food Science and Technology International, Tokyo 3, 348–352. http://joi.jlc.jst.go.jp/JST.JSTAGE/fsti9596t9798/3.348?from=CrossRef. https://www.jstage.jst.go.jp/article/fsti9596t9798/3/4/3{_}4{_}348/{_}pdf, doi:10.3136/fsti9596t9798.3.348.

Meiwa Co. Ltd, 2018. Meiwa co., Ltd. https://www.meiwa-ind.co.jp/en/products/product-06/.

Miyawaki, O., Liu, L., Nakamura, K., 1998. Effective partition constant of solute between ice and liquid phases in progressive freeze-concentration. J. Food Sci. 63, 756–758. https://doi.org/10.1111/j.1365-2621.1998.tb17893.x http://doi.wiley.com/10.1111/j.1365-2621.1998.tb17893.x.

Miyawaki, O., Liu, L., Shirai, Y., Sakashita, S., Kagitani, K., 2005. Tubular ice system for scale-up of progressive freeze-concentration. J. Food Eng. 69, 107–113. http://linkinghub.elsevier.com/retrieve/pii/S0260877404003528. doi:10.1016/j.jfoodeng.2004.07.016.

Moreno, F., Raventós, M., Hernández, E., Ruiz, Y., 2014. Block freeze-concentration of coffee extract: effect of freezing and thawing stages on solute recovery and bioactive compounds. J. Food Eng. 120, 158–166. https://www.sciencedirect.com/science/article/pii/S0260877413004007. doi:10.1016/J.JFOODENG.2013.07.034.

Myerson, A.S., Erdemir, D., Lee, A., 2019. Handbook of Industrial Crystallization, third ed. ed. Cambridge University Press, Cambridge https://www.cambridge.org/core/product/identifier/9781139026949/type/book. https://doi.org/10.1017/9781139026949 http://public.ebookcentral.proquest.com/choice/publicfullrecord.aspx?p=5928442, doi:10.1017/9781139026949.

Ojeda, A., Moreno, F.L., Ruiz, R.Y., Blanco, M., Raventós, M., Hernández, E., 2017. Effect of process parameters on the progressive freeze concentration of sucrose solutions. Chem. Eng. Commun. 204, 951–956. https://doi.org/10.1080/00986445.2017.1328413 doi:10.1080/00986445.2017.1328413.

Petzold, G., Moreno, J., Lastra, P., Rojas, K., Orellana, P., 2015. Block freeze concentration assisted by centrifugation applied to blueberry and pineapple juices, 30. Innovative Food Science & Emerging Technologies, pp. 192–197. https://www.sciencedirect.com/science/article/pii/S1466856415000569. doi:10.1016/J.IFSET.2015.03.007.

Pradistsuwana, C., Theprugsa, P., Miyawaki, O., 2003. Measurement of limiting partition coefficient in progressive freeze-concentration. Food Sci. Technol. Res. 9, 190–192. http://joi.jlc.jst.go.jp/JST.JSTAGE/fstr/9.190?from=CrossRef. doi:10.3136/fstr.9.190.

Rane, M.V., Jabade, S.K., 2005. Freeze concentration of sugarcane juice in a jaggery making process. Appl. Therm. Eng. 25, 2122–2137. https://www.sciencedirect.com/science/article/pii/S1359431105000608. doi:10.1016/J.APPLTHERMALENG.2005.01.014.

Ratkje, S.K., Flesland, O., 1995. Modelling the freeze concentration process by irreversible thermodynamics. J. Food Eng. 25, 553–568 doi:10.1016/0260-8774(94)00034-7.

Raventós, M., Hernández, E., Auleda, J., Ibarz, A., 2007. Concentration of aqueous sugar solutions in a multi-plate cryoconcentrator. J. Food Eng. 79, 577–585. http://linkinghub.elsevier.com/retrieve/pii/S0260877406001932. doi:10.1016/j.jfoodeng.2006.02.017.

Roos, Y., Karel, M., 1991a. Amorphous state and delayed ice formation in sucrose solutions. Int. J. Food Sci. Technol. 26, 553–566. https://doi.org/10.1111/j.1365-2621.1991.tb02001.x http://doi.wiley.com/10.1111/j.1365-2621.1991.tb02001.x.

Roos, Y., Karel, M., 1991b. Phase transitions of amorphous sucrose and frozen sucrose solutions. J. Food Sci. 56, 266–267. https://doi.org/10.1111/j.1365-2621.1991.tb08029.x http://doi.wiley.com/10.1111/j.1365-2621.1991.tb08029.x.

Roos, Y.H., 2010. Glass transition temperature and its relevance in food processing. Annual Review of Food Science and Technology 1, 469–496. https://doi.org/10.1146/annurev.food.102308.124139 http://www.annualreviews.org/doi/10.1146/annurev.food.102308.124139, doi:10.1146/annurev.food.102308.124139.

Sánchez, J., Hernández, E., Auleda, J., Raventós, M., 2011. Freeze concentration of whey in a falling-film based pilot plant: process and characterization. J. Food Eng. 103, 147–155. https://www.sciencedirect.com/science/article/pii/S0260877410004978. doi:10.1016/J.JFOODENG.2010.10.009.

Scholz, R., 1993. Die Schichtkristallisation Als Thermisches Trennverfahren. Ph.D. thesis. Universitat Bremen, Dusseldorf.

Scholz, R., Wangnick, K., Ulrich, J., 1993. On the distribution and movement of impurities in crystalline layers in melt crystallization processes. J. Phys. Appl. Phys. 26, B156–B161. http://stacks.iop.org/0022-3727/26/i=8B/a=025?key=crossref.a6f8fe8e0a886fd757698c1f69f83ab4. doi:10.1088/0022-3727/26/8B/025.

Shampine, L.F., Reichelt, M.W., 1997. The MATLAB ODE suite. SIAM J. Sci. Comput. 18, 1–22. https://doi.org/10.1137/S1064827594276424 doi:10.1137/S1064827594276424.

Shen, J.L., 1976. Solubility profile, intrinsic viscosity, and optical rotation studies of acid precipitated soy protein and of commercial soy isolate. J. Agric. Food Chem. 24, 784–788. https://doi.org/10.1021/jf60206a044 doi:10.1021/jf60206a044.

van der Sman, R., 2016. Phase field simulations of ice crystal growth in sugar solutions. Int. J. Heat Mass Tran. 95, 153–161 doi:10.1016/J.IJHEATMASSTRANSFER.2015.11.089 https://www.sciencedirect.com/science/article/pii/S0017931015300442?via{%}3Dihub{#}b0105.

van der Sman, R.G.M., 2017. Predicting the solubility of mixtures of sugars and their replacers using the Flory-Huggins theory. Food & Function 8, 360–371. https://doi.org/10.1039/C6FO01497F doi:10.1039/C6FO01497F.

van der Sman, R.G.M., Mauer, L.J., 2019. Starch gelatinization temperature in sugar and polyol solutions explained by hydrogen bond density. Food Hydrocolloids 94, 371–380. http://www.sciencedirect.com/science/article/pii/S0268005X19303194. doi:https://doi.org/10.1016/j.foodhyd.2019.03.034.

Vuist, J.E., Boom, R.M., Schutyser, M.A.I., 2020. Solute inclusion and freezing rate during progressive freeze concentration of sucrose and maltodextrin solutions. Dry. Technol. 1–9. https://www.tandfonline.com/doi/full/10.1080/07373937.2020.1742151. doi:10.1080/07373937.2020.1742151.

Williams, M.L., Landel, R.F., Ferry, J.D., 1955. The temperature dependence of relaxation mechanisms in amorphous polymers and other glass-forming liquids. J. Am. Chem. Soc. 77, 3701–3707. https://doi.org/10.1021/ja01619a008 doi:10.1021/ja01619a008.